Electronic Supplementary Material (ESI) for Inorganic Chemistry Frontiers.
This journal is © the Partner Organisations 2024

Unlocking Fast Kinetics of n-p-Type Heterostructured MoS_2@PANI Photocathode toward Robust Low-Overpotential Li-O_2 Battery

Shuanghong Xia[#], Yang Yang[#], Qingzheng Jia, Mengyao Shang, Ling Li*, Song Chen*, Wenming Zhang*.

Province-Ministry Co-construction Collaborative Innovation Center of Hebei Photovoltaic Technology, College of Physics Science and Technology, Hebei University, Baoding 071002, China.

Corresponding Author

E-mail: lilinghbu@163.com (L. Li), songchen@hbu.edu.cn (C. Song), wmzhanghbu@126.com (W. Zhang).

[#]The authors contribute equally.

1. Material and Methods

1.1 Materials. $(NH_4)_6Mo_7O_{24}\cdot 4H_2O$ (Aladdin, Shanghai, China), CH_4N_2S (Aladdin, Shanghai, China), Aniline (Aladdin, Shanghai, China), $(NH_4)_2S_2O_8$ (Aladdin, Shanghai, China), HCl (Aladdin, Shanghai, China).

1.2 Material preparation.

Preparation of MoS_2. 1.359 g of ammonium molybdate and 2.512 g of thiourea were dissolved in 38 ml of deionized water. After dissolving and stirring for 30 min, it was poured into a polytetrafluoroethylene hydrothermal kettle and hydrothermally heated at 200°C for 24 h. The precipitate was collected and cleaned with deionized water and ethanol, and dried for 24 h under vacuum.

Preparation of PANI. Dissolve 0.3 ml of aniline and 0.18 g of ammonium persulfate in 12 ml of HCl (1 mol/L). It was stirred strongly for 30 min, and after discoloration, ice bath for 12h (under the condition of avoiding light). The precipitate was collected and washed hurriedly with deionized water and lyophilize for 24h.

Preparation of MoS_2@PANI. The prepared 0.5 g of PANI and 0.125 g of MoS_2 were dispersed in 24 ml of HCl (1 mol/L) solution. After ultrasonic crushing for 10 min, it was hydrothermally heated at 120°C for 18 h. The precipitate was washed with deionized water and the product was collected by lyophilization for 24 h.

1.3 Material characterizations.

The microstructures of the complexes were observed by field emission scanning electron microscopy (SEM, MAGELLAN-400) and transmission electron microscopy (TEM, JEM-1011). The prepared products were tested with a Bruker AXS D8 advanced

X-ray diffractometer (XRD) over the 2θ range of 10 to 80°.

1.4 Electrochemical measurements.

Assembly of the MoS_2@PANI cathode cells was carried out in a glove box (O_2 < 0.1 ppm, H_2O < 0.1 ppm). The MoS_2@PANI, conductive agent (acetylene black), and binder (PVDF) were mixed with a ratio of 7:2:1 to form a slurry, and a dispersant was added to the slurry. After stirring for 12 h，the slurry was uniformly spread on carbon clothe with an electric roller and dried at 60°C. 1.0 M lithium bis (trifluoromethanesulfonyl)imide (LiTFSI) in tetraethylene glycol dimethyl ether (TEGDME) as the electrolyte. The Li foil was used as the reference electrode. A glass microfiber filter (Whatman GF/D) was used as the separator. The assembled cathode shell of the cell had 8mm diameter holes for receiving light and was placed in a homemade transparent sealed box filled with oxygen. After oxygen purging for 30min, constant current charge/discharge tests were performed with a cell test system (Land CT2001A). Cyclic voltammetry (CV) and electrochemical impedance spectroscopy (EIS) were performed with an electrochemical workstation (CHI 660E).

1.5 DFT Calculations

We have employed the first-principles [1,2] to perform density functional theory (DFT) calculations within the generalized gradient approximation (GGA) using the Perdew-Burke-Ernzerhof (PBE) [3] formulation. We have chosen the projected augmented wave (PAW) potentials [4,5] to describe the ionic cores and take valence electrons into account using a plane wave basis set with a kinetic energy cutoff of 450eV. Partial occupancies of the Kohn−Sham orbitals were allowed using the

Gaussian smearing method and a width of 0.05 eV. The electronic energy was considered self-consistent when the energy change was smaller than 10^{-5} eV. A geometry optimization was considered convergent when the energy change was smaller than 0.05 eV $Å^{-1}$. The vacuum spacing in a direction perpendicular to the plane of the structure is 18 Å for the surfaces. The Brillouin zone integration is performed using 2×2×1 Monkhorst-Pack k-point sampling for a structure. Finally, the adsorption energies (Eads) were calculated as Eads= Ead/sub-Ead-Esub, where Ead/sub, Ead, and Esub are the total energies of the optimized adsorbate/substrate system, the adsorbate in the structure, and the clean substrate, respectively. For the exciton, the higher spin-up state is occupied by the spin-up electron from the VBM. With the occupation of these electronic states fixed, the structural relaxation will be calculated.

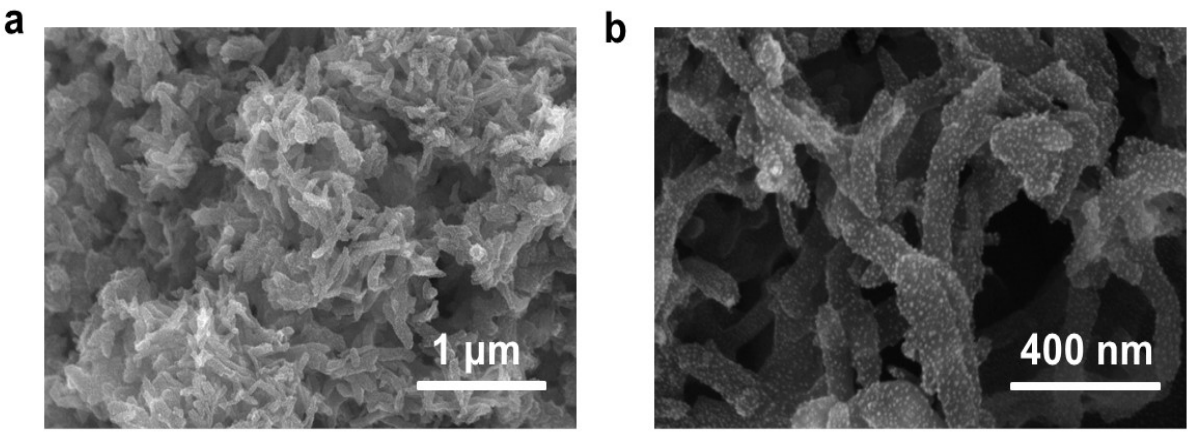

Fig. S1 SEM images of (a, b) pure PANI.

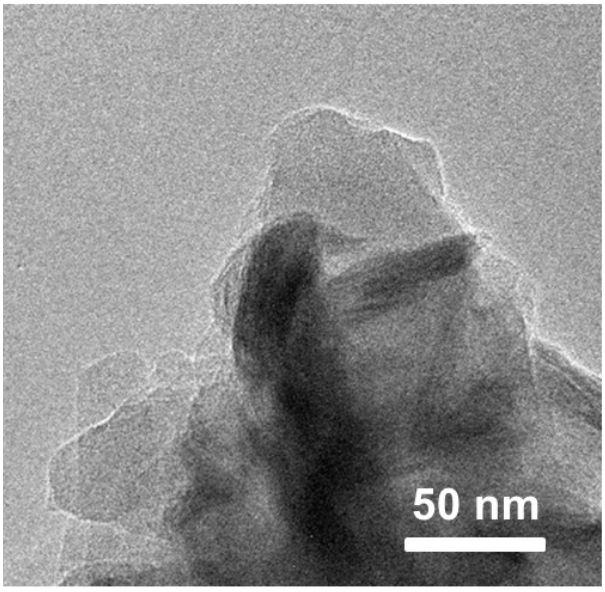

Fig. S2 TEM image of PANI@MoS_2.

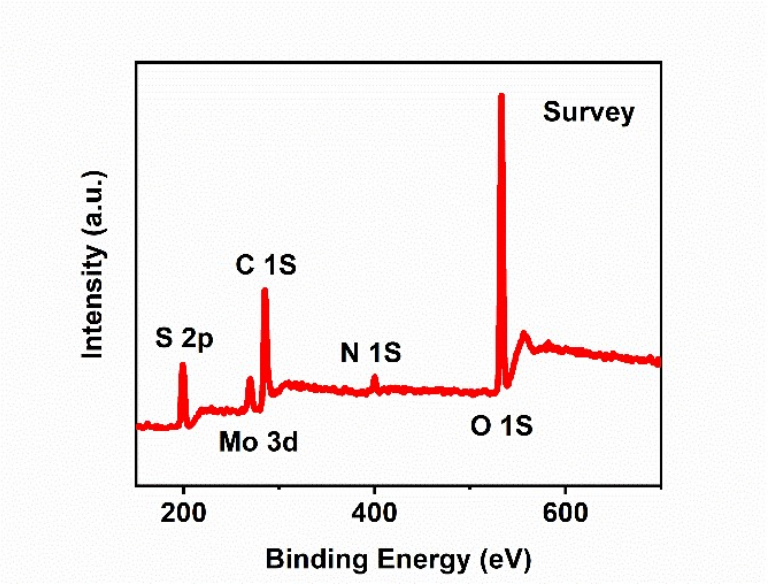

Fig. S3 Full chromatogram of PANI@MoS_2.

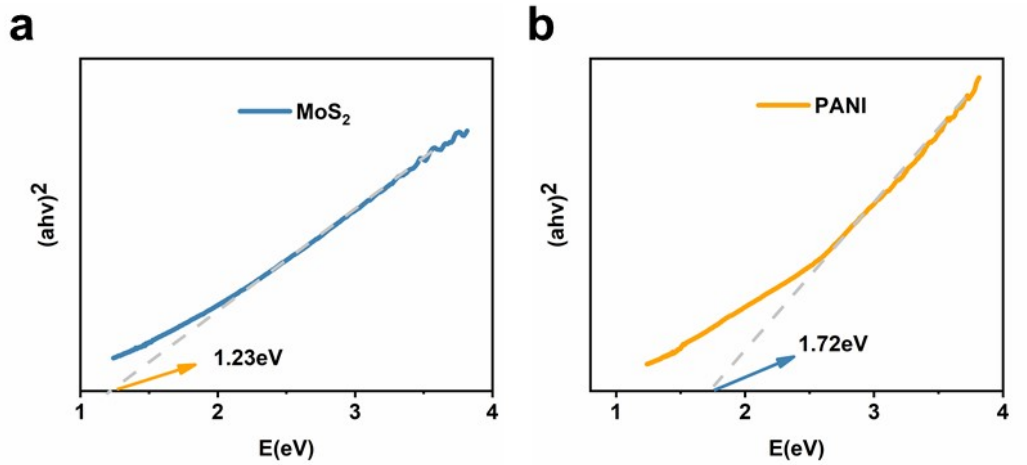

Fig. S4 Tauc plot curves of (a) MoS_2 and (b) PANI.

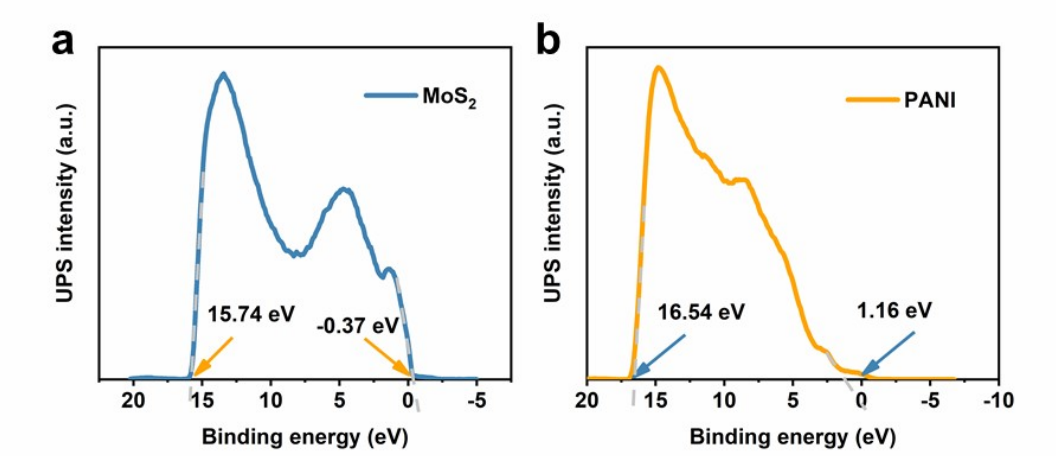

Fig. S5 UPS spectra of the (a) MoS_2 and (b) PANI.

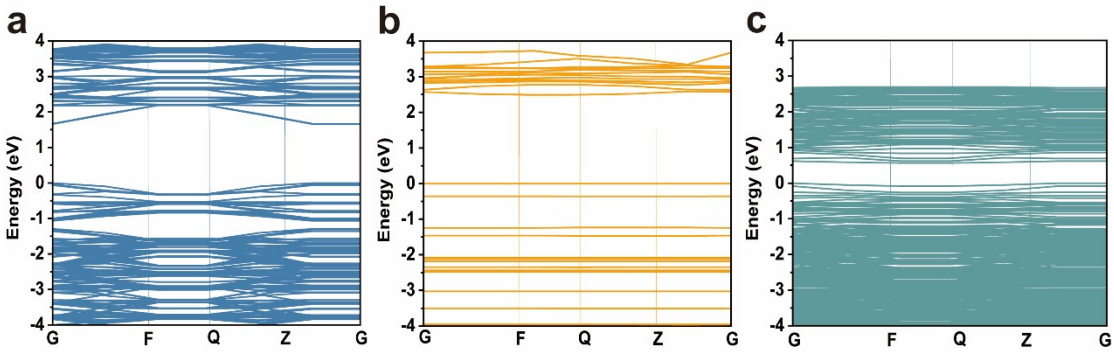

Fig. S6 the calculated band structure of the (a) MoS_2, (b)PANI and (c) MoS_2@PANI.

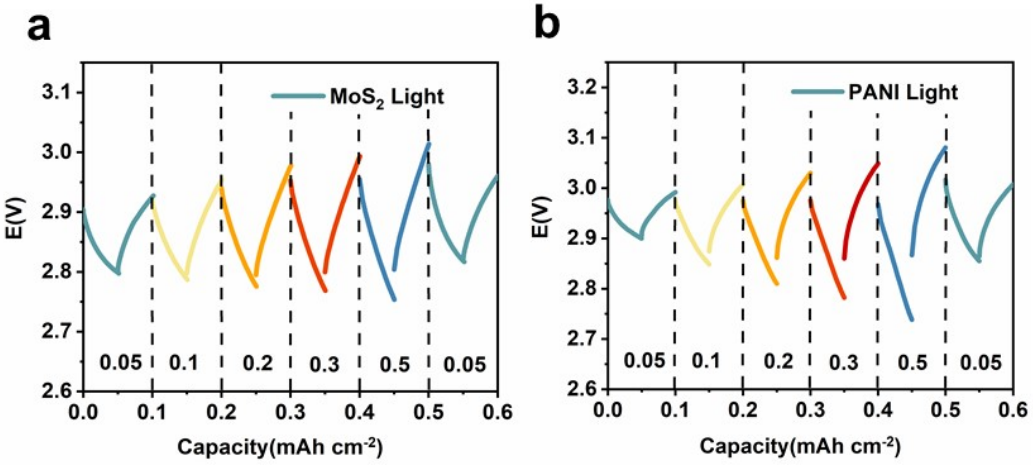

Fig. S7 Discharge/charge curves at varied currents with illumination of the (a) MoS_2 and (b) PANI.

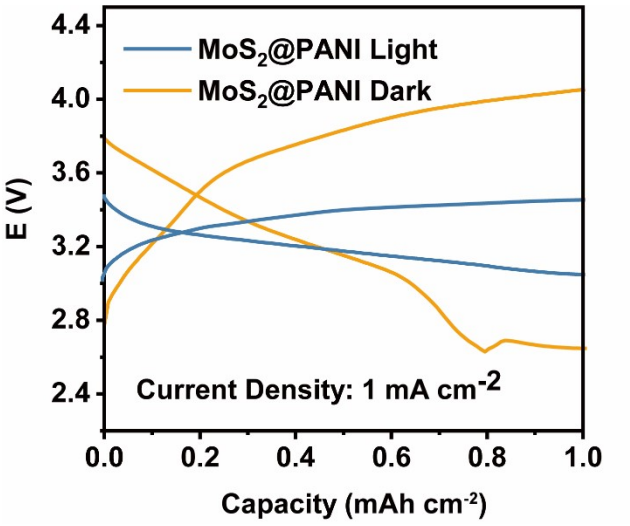

Fig. S8 Charge/discharge profiles at current densities of 1 mA cm^{-2} and cutoff capacities of 1 mAh cm^{-2}.

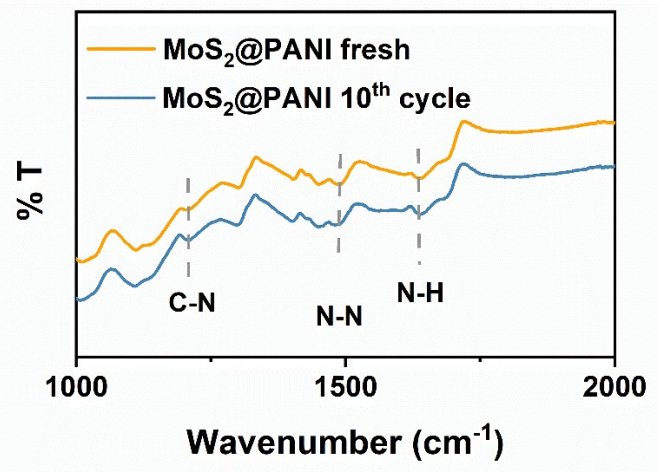

Fig. S9 FTIR spectra of the MoS_2@PANI electrodes before and after 10 cycles.

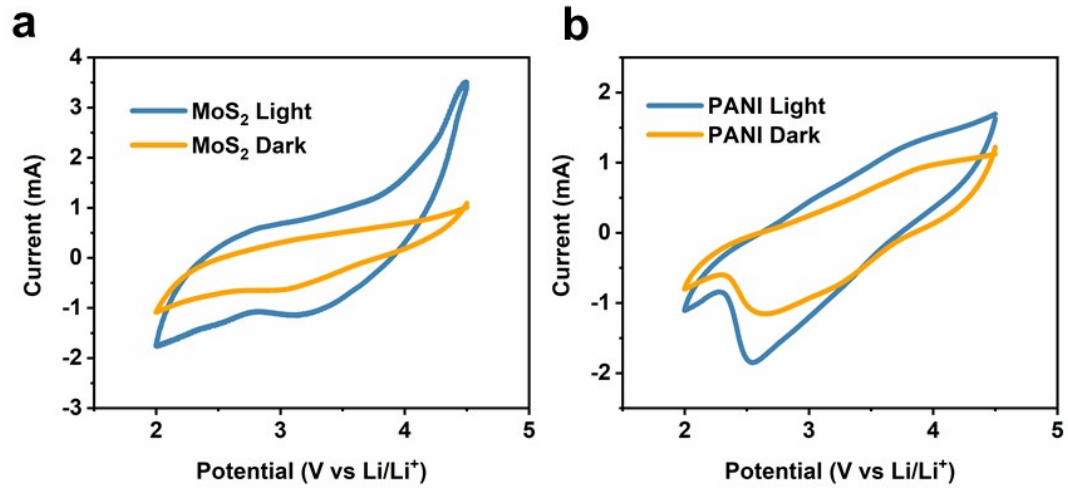

Fig. S10 CV curves with and without illumination of the (a) MoS_2 and (b) PANI.

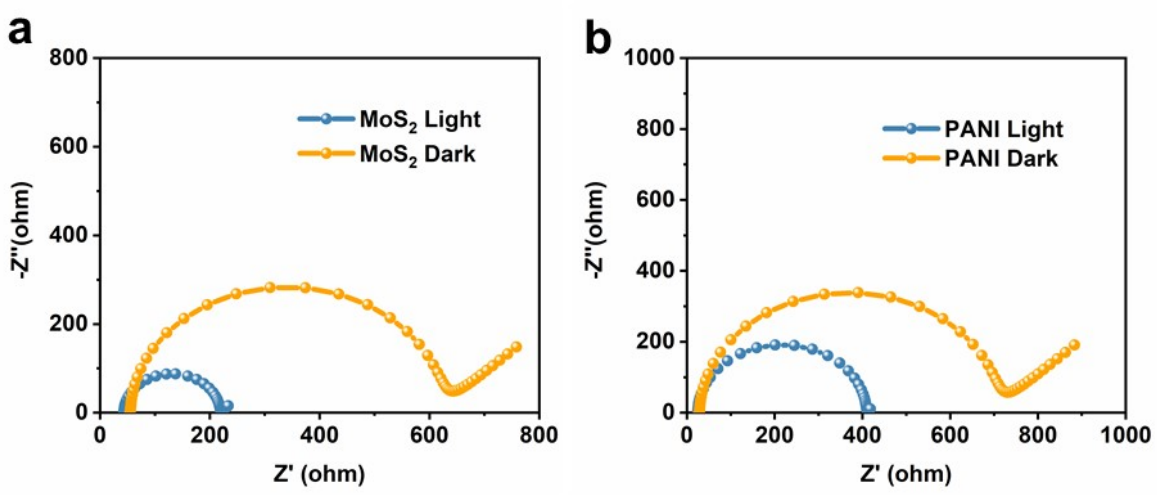

Fig. S11 Nyquist plots with and without illumination of the (a) MoS_2 and (b) PANI.

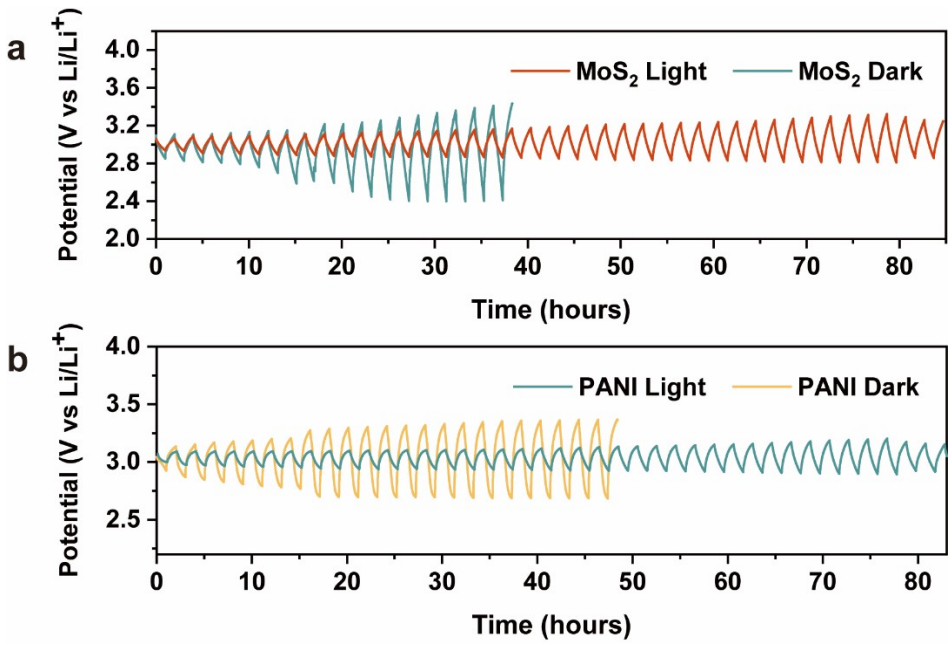

Fig. S12 Long cycle electrochemical performance of individual (a) MoS_2 and (b) PANI with and without illumination.

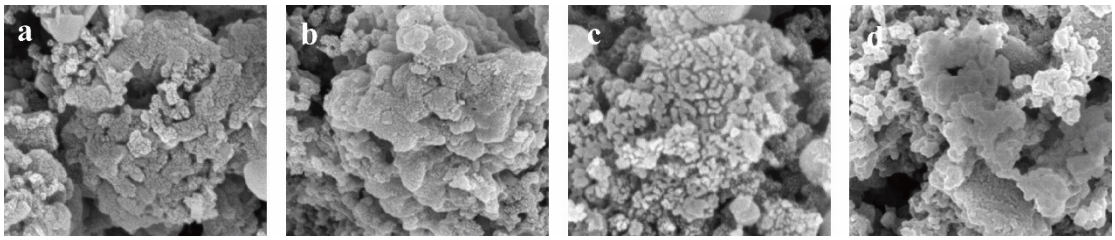

Fig. S13 SEM images of different durations of discharge: (a) 0.5h, (b) 1h, (c) 2h and (d) 5h.

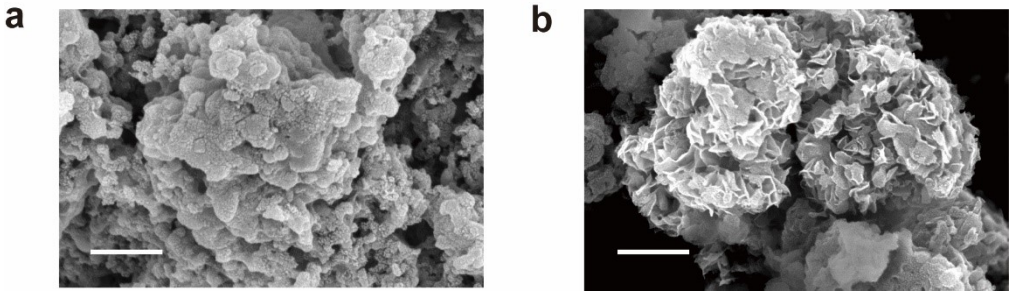

Fig. S14 SEM images of the discharged and recharged MoS_2@PANI cathodes (scale bar: 500 nm).

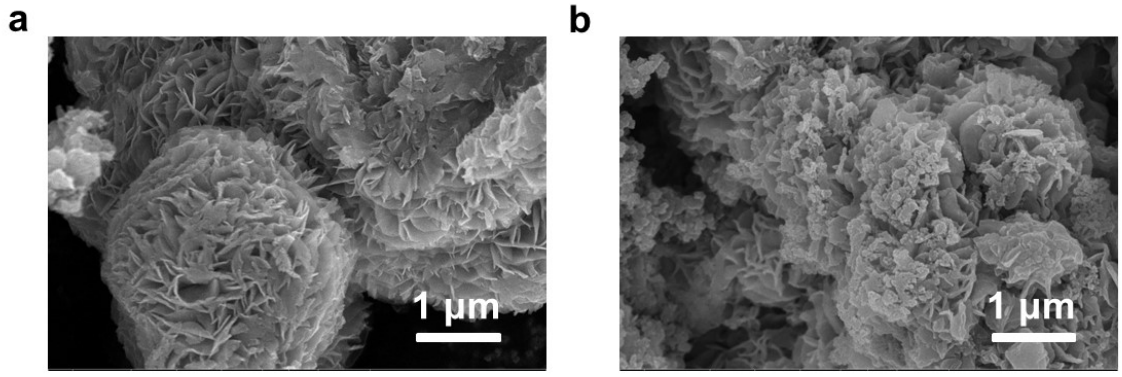

Fig. S15 SEM images of different durations of discharge: (a) Fresh, (b) 1h.

Table S1 Comparison of the electrochemical performances of MoS_2@PANI with reported cathode materials for Li-O_2 batteries.

Materials	Discharge Voltage (V)	Charge Voltage (V)	Current density (mA cm^{-2})	Energy Efficiency	Ref
MoS_2 /$ZnIn_2S_4$	3.22	3.25	0.02	99.1%	[6]
	3.17	3.29	0.05	96%	
	3.13	3.45	0.2	90.7%	
TiO_2 /Fe_2O_3	3.12	3.2	0.01	97.5%	[7]
	~2.84	~3.75	0.05	75.7%	
$CsPbBr_3$@ PCN-333	3.19	3.44	0.01	92.7%	[8]
	~2.6	~3.7	0.2	70.2%	
Fe_2O_3	2.68	3.09	0.06	86.7%	[9]
	2.56	3.15	0.12	81.2%	
$CeVO_4$@C NT	~3	3.45	0.1	86.9%	[10]
	~2.98	~3.8	0.15	78.4%	
g-C_3N_4	3.22	3.38	0.1	95%	[11]
TiO_2	2.65	2.86	0.01	92%	[12]
ZnS	2.47	2.08	0.026	>100%	[13]
g-C_3N_4, I_2/I_{3-}	2.7	1.9	0.01	>100%	[14]
Au-SnO_2	3.10	3.59	100 mA g^{-1}	86.3%	[15]
MoS_2@PANI	3.18	3.26	0.05	97.5%	This work

References

[1] G. Kresse, J. Furthmüller, Efficiency of Ab-Initio Total Energy Calculations for Metals and Semiconductors Using a Plane-Wave Basis Set, Comput. Mater. Sci. 6 (1996) 15-50.

[2] G. Kresse, J. Furthmüller, Efficient Iterative Schemes for Ab Initio Total-Energy Calculations Using a Plane-Wave Basis Set, Phys. Rev. B. 54 (1996) 11169-11186.

[3] J.P. Perdew, K. Burke, M. Ernzerhof, Generalized Gradient Approximation Made Simple, Phys. Rev. Lett. 77 (1996) 3865-3868.

[4] G. Kresse, D. Joubert, From Ultrasoft Pseudopotentials to the Projector Augmented-Wave Method, Phys. Rev. B. 59 (1999) 1758-1775.

[5] P.E. Blöchl, Projector Augmented-Wave Method, Phys. Rev. B. 50 (1994) 17953-17979.

[6] H. Gong, T. Wang, K. Chang, P. Li, L.Q. Liu, X.Y. Yu, B. Gao, H.R. Xue, R.Z. Ma, J.P. He, J.H. Ye, Revealing the illumination effect on the discharge products in high-performance Li-O_2 batteries with heterostructured photocatalysts, Carbon Energy 4 (2022) 1169-1181.

[7] M.L. Li, X.X. Wang, F. Li, L.J. Zheng, J.J. Xu, J.H. Yu, A Bifunctional Photo-Assisted Li-O_2 Battery Based on a Hierarchical Heterostructured Cathode, Adv. Mater. 32 (2020).

[8] G.Y. Qiao, D.H. Guan, S. Yuan, H. Rao, X. Chen, J.A. Wang, J.S. Qin, J.J. Xu, J.H. Yu, Perovskite Quantum Dots Encapsulated in a Mesoporous Metal-Organic Framework as Synergistic Photocathode Materials, J. Am. Chem. Soc. 143 (2021)

14253-14260.

[9] H. Gong, H.R. Xue, B. Gao, Y. Li, X.L. Fan, S.T. Zhang, T. Wang, Introduction of photo electrochemical water-oxidation mechanism into hybrid lithium-oxygen batteries, Energy Stor. Mater. 31 (2020) 11-19.

[10] D.W. Li, X.Y. Lang, Y. Guo, Y.Q. Wang, Y.Y. Wang, H.C. Shi, S.C. Wu, W.C. Wang, Q.H. Yang, A photo-assisted electrocatalyst coupled with superoxide suppression for high performance Li-O_2 batteries, Nano Energy 85 (2021).

[11] Z. Zhu, X.M. Shi, G.L. Fan, F.J. Li, J. Chen, Photo-energy Conversion and Storage in an Aprotic Li-O_2 Battery, Angew. Chem. Int. Ed. 58 (2019) 19021-19026.

[12] H. Gong, T. Wang, H.R. Xue, X.L. Fan, B. Gao, H.B. Zhang, L. Shi, J.P. He, J.H. Ye, Photo-enhanced lithium oxygen batteries with defective titanium oxide as both photo-anode and air electrode, Energy Stor. Mater. 13 (2018) 49-56.

[13] Y. Liu, J. Yi, Y. Qiao, D. Wang, P. He, Q. Li, S.C. Wu, H.S. Zhou, Solar-driven efficient Li_2O_2 oxidation in solid-state Li-ion O_2 batteries, Energy Stor. Mater. 11 (2018) 170-175.

[14] Y. Liu, N. Li, S.C. Wu, K.M. Liao, K. Zhu, J. Yi, H.S. Zhou, Reducing the charging voltage of a Li-O_2 battery to 1.9 V by incorporating a photocatalyst, Energy Environ. Sci. 8 (2015) 2664-2667.

[15] W.X. Yang, F. Li, H.L. Liu, Z. Li, J.Q. Zhao, Y. Wang, Boosting the electrochemistry of Li_2O_2 in lithium-oxygen batteries by plasmon-induced hot-electron injection, New J. Chem. 45 (2021) 21160-21167.